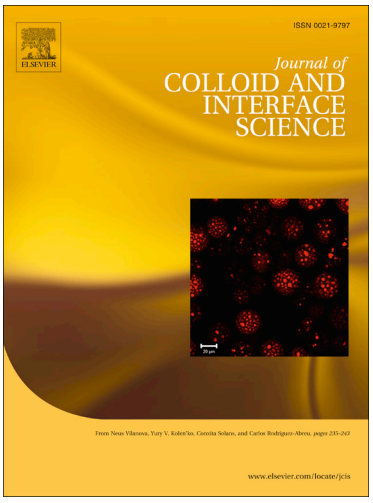

Magnetic Ugi-Functionalized Graphene Oxide Complexed with Copper Nanoparticles: Efficient Catalyst toward Ullman Coupling Reaction in Deep Eutectic Solvents

Ahmad Shaabani, Ronak Afshari

PII: S0021-9797(17)31120-7
DOI: https://doi.org/10.1016/j.jcis.2017.09.089
Reference: YJCIS 22841

To appear in: *Journal of Colloid and Interface Science*

Received Date: 25 July 2017
Revised Date: 21 September 2017
Accepted Date: 22 September 2017

Please cite this article as: A. Shaabani, R. Afshari, Magnetic Ugi-Functionalized Graphene Oxide Complexed with Copper Nanoparticles: Efficient Catalyst toward Ullman Coupling Reaction in Deep Eutectic Solvents, *Journal of Colloid and Interface Science* (2017), doi: https://doi.org/10.1016/j.jcis.2017.09.089

Magnetic Ugi-Functionalized Graphene Oxide Complexed with Copper Nanoparticles: Efficient Catalyst toward Ullman Coupling Reaction in Deep Eutectic Solvents

Ahmad Shaabani∗and Ronak Afshari

Faculty of Chemistry, Shahid Beheshti University, G. C., P. O. Box 19396-4716, Tehran, Iran

∗ Corresponding author. Tel.: +982129902800; e-mail: a-shaabani@sbu.ac.ir

Abstract

Herein, we report the direct synthesis of carboxamide-functionalized graphene oxide (carboxamide-*f*-GO) for the development of new nanocatalysts, with highly dispersed particles, through covalent functionalization with a facile and direct strategy. This surface functionalization was carried out through a one-pot sequential four-component Ugi reaction. Subsequently, the Ugi-ligand decorated on the surface of the graphene oxide sheets coordinated with copper nanoparticles (Cu NPs) and finally covered with magnetic nanoparticles. The synthesized nanocatalyst was characterized by Fourier transform infrared (FT-IR), proton nuclear magnetic resonance spectroscopy (^{1}H NMR), X-ray powder diffraction (XRD), scanning electron microscopy (SEM), energy-dispersive X-ray spectroscopy (EDX), dynamic light scattering (DLS), thermogravimetric analysis (TGA) and atomic force microscopy (AFM). The carboxamido nitrogen in Ugi-ligand showed high affinity toward complexation with Cu NPs and has a profound effect on the reactivity of the copper center in this nanocatalyst. The catalytic activity of nanocatalyst was investigated in Ullmann cross-coupling reaction for practical and direct access to corresponding *N*-aryl amines in a deep eutectic solvent as a green and recyclable media. The results showed the capability of this designed catalytic system through *N*-arylation of *N*-heterocycles and aniline derivatives with high yields in short reaction times. In addition, both of the nanocatalyst and deep eutectic solvent were easily recovered and reused for five consecutive runs.

Keyword: Graphene oxide, Ugi four-component reaction, Nanocatalyst, Deep eutectic solvent, Ullman C-N coupling, Dispersity

Introduction

A dramatic rise in interest has occurred since the discovery of graphene with regards to graphene-based nanomaterials [1]. Graphene consists of single-layer-thick sheets of sp^2 bonded carbon atoms that are arranged in a two-dimensional (2D) honeycomb network [2]. Considering to this structure, graphene shows a number of unique and extraordinary structural, electronic, and optical properties [3-7]. These unparalleled properties include a high surface area, predominant mechanical strength, thermal conductivity and so forth [8, 9]. Eventually, these great potentials have been conducted to wide interdisciplinary applications of graphene in various fields such as sensors, drug delivery, electronic and catalyst to name a few [10-14].

Functionalization reactions are reactions that introduced desired groups on the surface of materials, based on the oxidation reactions and later can lead to the other functional groups [15, 16]. Graphene, one of the most important carbonaceous materials, has been functionalized frequently to produce graphene oxide (GO) that showed robust ability to yield further manifold functional nanomaterials [17]. Among various such fields, the research in functionalized graphene-based nanomaterials as a catalyst is still in its infancy since exponentially upward trend recently [18, 19]. Besides, derivatization reactions are reactions in which the induced functional group on the surface of materials is involved in the subsequent reactions. In the case of graphene-derivatization, the chemical structure and complex functions are bonded to the graphene to add more functionality and attachment of various metal and metal oxide nanoparticles to the surface for further use as an efficient metal-functionalized graphene nanocomposite [20-22].

On the other hand, small synthetic ligands are appropriate alternatives due to their robustness, low synthetic cost and fast ligand development [23]. The carboxamide [–C(O)NH–] group, a crucial building block in the primary structure of proteins, is a vital ligand unit for coordination chemists [24]. Transition metal coordination by a carboxamide oxygen is occasionally observed in native enzymes such as kidney bean purple acid phosphatase and serine/threonine protein phosphatase-1 [25]. Recently, graphene oxide functionalized with carboxamide ligands appear in amino acids possessing copper affinity have been assembled by chemical functionalization, producing an excellent catalyst for the epoxidation of norbornene [26].

Isocyanide-based multicomponent reactions (I-MCRs), for their intimate nature, produce a high increase of molecular complexity in a one-pot procedure, which caused a high degree of atomic economy, high number of bond-forming (bond-forming economy), and the stereochemical diversity [27, 28]. Among all the I-MCRs, special attention must be given to a Ugi four-component reaction and also abbreviated as Ugi-4CR [29]. The Ugi 4-CR allows the synthesis of diversely substituted pseudo-peptides with carboxamide functionality [30, 31]. Recently, the union of materials chemistry with multicomponent approaches has accelerated the preparation of novel functional materials. These innovative strategies have

many advantages such as operational simplicity, substrate diversity and in particular, pot, atom and step economic feature which caused to some of the adequate aspects of green chemistry; reduced cost, low waste and pollutant productions. Very recently, Ugi-4CR has been used for the synthesis of novel carbonaceous-based drug or gene carriers [32-34]. The development of novel functionalized materials with MCR approach as a catalyst remains a significant challenge; therefore it is highly desirable to assess their efficiency and applicability in the construction of a nanocatalyst for organic transformations.

Aromatic carbon-nitrogen bond formations have been prepared by Ullmann-type cross-coupling of heterocyclic nitrogen compounds or primary and secondary amines with aryl halides through copper nanoparticles [35-37]. Since the classic Ullman reaction needs harsh reaction conditions and stoichiometric amounts of copper for overcoming these drawbacks a recent notable achievement has been developed for the utilization of various copper-chelating ligands. However, most of these protocols suffer from limitations such as weak reusability of the catalysts and utilizing of toxic ligands. Thus, the development of a mild and efficient catalytic procedure for the amination of aryl halides with eco-compatible conditions is highly desirable.

One of the important issues in green chemistry is embedment of conventional toxic organic solvents with eco-friendly non-toxic alternatives that do not have flammable vapors at a wide range of temperature. In this regards, deep eutectic solvents (DESs) as green, bio-renewable, and biodegradable solvents have gained significant attention in the recent years. DESs have a non-toxicity, non-volatility, inflammability and a wider liquid temperature range and also can be sourced from renewable feed stocks, with a cheap production procedure [38]. The most studied series of DESs are those prepared using choline chloride as a donor compound with components including urea, glycerol, carboxylic acids, and ethylene glycol or metal salts such as $FeCl_3$ [39]. Owing to these advantages, DESs have gained a growing interest in many fields of research such as organic synthesis, pharmaceutical applications, surfactant chemistry, extraction processes, polymerization, electrochemistry and functional materials [40, 41].

In view of our current interest in preparation and application of functionalized materials [42-44] and development of Ugi reactions [34, 45, 46], herein, we developed the utilization of Ugi-4CR as a tailored multicomponent ligation approach towards the synthesis of carboxamide-ligands chemically grafted on the surface of graphene nanosheets (carboxamide-*f*-GO), for first time, leading to the novel nanocatalyst which have high affinity to complex with copper nanoparticles (Cu NP-carboxamide-*f*-GO). In order to make a nanocatalyst reusable, the Fe_3O_4 nanoparticles (Fe_3O_4 NPs) were synthesized on the surface of nanomaterial to yield final Cu NP-carboxamide-*f*-GO@Fe_3O_4 nanocomposite (@Fe_3O_4 means covered with Fe_3O_4 NPs). The application of nanocatalyst for rapid access to corresponding *N*-aryl amines was investigated in a benign deep eutectic solvent, which is a new generation of pioneer green solvents (Scheme 1).

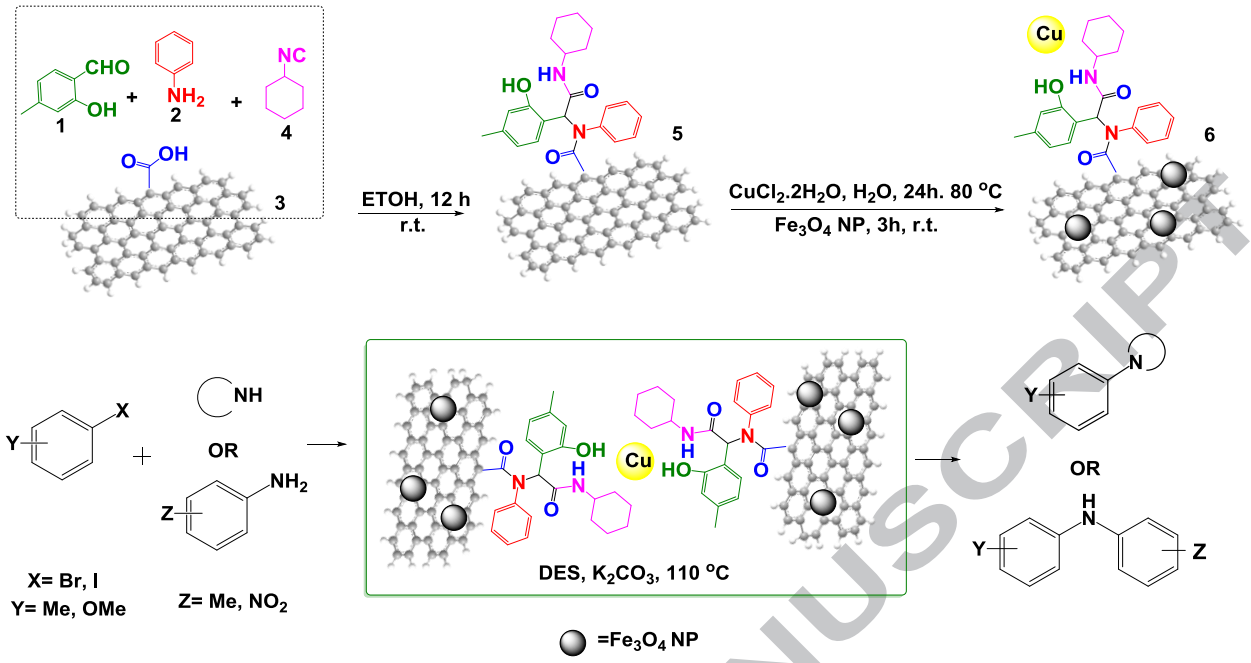

Scheme 1 Synthesis of Cu NP-carboxamide-*f*-GO@Fe_3O_4 *via* a four-component Ugi reaction for C-N bond formation trough Ullmann cross-coupling reactions

Experimental

1-General

Graphite flake with an average lateral size of 20-100 micron was purchased from Merck. All reagents were purchased from Merck and Aldrich and used without further purification. The X-ray diffraction (XRD) pattern of the carbonaceous nanomaterials was recorded on a diffractometer (STOE & CIE STADI P) with a scintillation detector. Scanning electron microscopy (SEM) observations were carried out using an environmental scanning electron microscope (Philips XL30 ESEM). Atomic force microscopy (AFM) images were obtained using a Nanosurf Mobile S atomic force microscope with the non-contact mode. The polydispersity index (PdI) was measured by dynamic light scattering (DLS) (Zetasizer Nano ZS90, Malvern Instruments). Thermogravimetric analysis (TGA) was carried out using a simultaneous thermal analyzer (Scinco STA 1500) at a heating rate of 10 °C min^{-1} in the air. Fourier transform infrared (FT-IR) spectra were made in KBr pellets on a Shimadzu IR470 spectrometer. The amount of Cu nanoparticles was estimated using an inductively coupled plasma optical emission spectrometer (ICP-OES; Varian Vista PRO Radial). The elemental analyses were performed with an Elementar Analysensysteme GmbH Vario EL. ^{1}H and ^{13}C NMR spectra were recorded on a BRUKER DRX-300 AVANCE spectrometer at 300.13 and 75.47 MHz. NMR spectra were obtained in $CDCl_3$.

2-Synthesis of the graphene oxide (GO)

GO was synthesized from natural graphite *via* preoxidation/thermal expansion of graphite followed by modified Hummer's method [37, 38]. At first step, 10 g of natural graphite flake was mixed with 3:1 volume ratio of H_2SO_4:HNO_3 for 24 h. Then 400 ml of water was added to the resultant solution for quenching the reaction. The resultant product was then filtered and washed out with water and dried under vacuum at 60 °C for 24 h. In the second step, 2 g of the product was mixed with 200 ml of H_2SO_4 and 6 g potassium permanganate for 24 h caused to a thick paste. Then, 600 ml of distilled water was added to the paste, and the reaction was terminated by addition of aqueous solution of 50 ml H_2O_2, resulting in a yellow brown mixture. Then the mixture was centrifuged and washed out three times with 10% HCl solution and then three times with distilled water. The procedure was followed by sonication for 30 minutes to produce GO stable aqueous dispersion. At the end of this process, the mixture was centrifuged for 15 min at 7000 rpm in order to remove un-exfoliated graphite oxide particles. The full characterization of synthesized GO is presented in the Supporting Information, Fig. S1.

3-General procedure for the preparation of carboxamide-functionalized graphene oxide (carboxamide-*f*-GO)

In a typical procedure, 2-hydroxy-4-methylbenzaldehyde (0.68 g, 5.00 mmol) and aniline (0.46 g, 5.00 mmol) were dissolved in EtOH (25 mL). The solution was stirred at room temperature for 30 min. Then, cyclohexyl isocyanide (0.54 g, 5.00 mmol) and GO (0.50 g) were added and the resulting mixture was stirred at 60 °C for 12 h in a closed vial. On completion, the reaction mixture was cooled to room temperature, and carboxamide-*f*-GO was easily purified by washing with ethanol/Acetone and isolated by centrifugation (20000 rpm, 10 min, 5 times).

4-Preparation of Cu NP-carboxamide-*f*-GO@Fe_3O_4

Carboxamide-*f*-GO (1.00 g) was dispersed in water and then ultrasonication was performed at room temperature. Then, a solution of $CuCl_2.2H_2O$ (0.09 g, 0.50 mmol) in 5 mL of H_2O was added dropwise to the reaction mixture, followed by the addition of ascorbic acid (50 mL, 0.05 M). The reaction mixture was stirred on a magnetic stirrer at 80 °C for 24 h. Then, Cu NP-carboxamide-*f*-GO were centrifuged and washed three times with deionized water (20000 rpm, 5 min, 3 times). The final step was the synthesis of the magnetic Fe_3O_4 using co-precipitation technique [47]. The Fe_3O_4 NPs (0.50 g) was dispersed in water (15 mL) and sonicated for 15 min then Cu NP-carboxamide-*f*-GO (1.00 g) added and sonication continued for 3 h at room temperature. Then, by applying an external magnet, the Cu NP-carboxamide-*f*-

$GO@Fe_3O_4$ were collected and then washed three times with deionized H_2O/ethanol and the magnetic precipitate was dried under vacuum at 60 °C.

5- Preparation of choline chloride-based deep eutectic solvent (DES)

Choline chloride-based deep eutectic solvent was prepared according to the literature [38, 48]. The two components were mixed on the basis of reported relationships showed in Table 1 and heated to 80 °C until a homogeneous colorless liquid was prepared. The obtained DESs were used without any further purification.

6-General procedure for the catalytic amination of aryl halides

A mixture of Cu NP-carboxamide-*f*-$GO@Fe_3O_4$ nanocomposite (0.05 mol % of Cu), K_2CO_3 (1.50 mmol), an amine (1.00 mmol) and an aryl halide (1.00 mmol) were placed in choline chloride–glycerol deep eutectic solvent (3 mL) and vigorously stirred at 110 °C for a certain period of time (0.5-3 h). After completion of the reaction as indicated by TLC (ethyl acetate and *n*-hexane), the reaction mixture was cooled to room temperature. Then, water (10 mL) was added; the catalyst was separated by an external magnet and diluted with ethyl acetate (10 mL). The insoluble crude product was filtered, concentrated and then the residue was purified by flash chromatography (SiO_2, ethyl acetate and *n*-hexane) to yield pure product.

7- **Statistical analysis**

All data are represented as means ± standard deviation (SD). The statistical analysis was performed using Origin Pro (version 8.5.1) at confidence levels of 95% and 99%.

Results and discussion

Graphene oxide was modified by further derivatization through Ugi-4CR to afford the Ugi-ligand with carboxamide scaffolds on the surface of graphene sheets. Distinct ability of carboxamide motifs to coordinate with transition metals, together with the advantages of covalent functionalization/derivatization approaches of graphene has prompted us to employ carboxylated graphene nanosheets (G-COOH) as an acid component in a Ugi four-component reaction for the synthesis of carboxamide functionalized graphene nanoparticles with the coordination ability of copper nanoparticles, for the first time. According to the commonly accepted Ugi reaction mechanism, the benzaldehyde **1**, aniline **2**, and GO **3** are in equilibrium with imine **[A]** in the reaction medium (Scheme 2). The addition of the cyclohexyl isocyanide **4** onto the iminium group followed by the addition of the carboxylate ion onto the C atom of the nitrilium ion leads to the formation of the adduct **[B]**, which

undergoes an intramolecular acylation known as Mumm rearrangement to give the stable carboxamide-*f*-GO **5**. Next, copper nanoparticles were immobilized onto the carboxamide coated surface of the GO. We used 2-hydroxy-4-methylbenzaldehyde due to the potentially ligand-active –OH groups which make the carboxamide scaffold appropriate bidentate ligands for metal chelates. Meanwhile, the quantitative determination of the copper content, as determined by ICP-OES was obtained to be 0.01mmol/g.

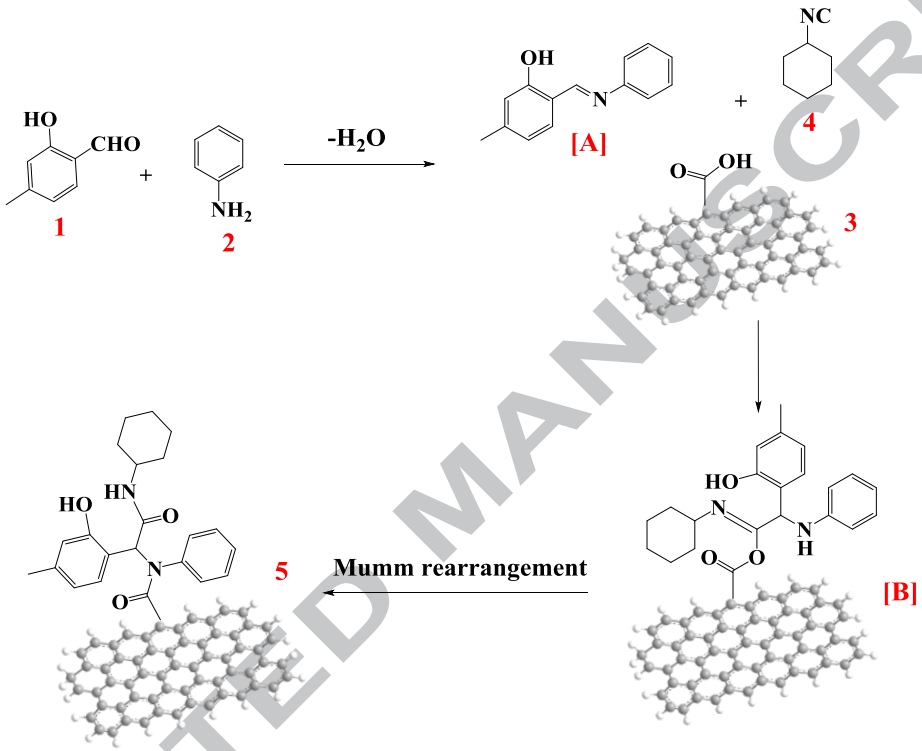

Scheme 2 Proposed mechanism for the synthesis of carboxamide-*f*-GO

The CHN analysis, before and after functionalization, confirm the existence of nitrogen atom originated from carboxamide scaffold on the surface of graphene sheets. The atomic percent of N_2 is 4.38 % which confirms the successful formation of amide bonds during the one-pot Ugi-4CR. The FT-IR spectra of carboxamide-*f*-GO and Cu NP-carboxamide-*f*-GO@Fe_3O_4 are shown in Fig. 1. In the FT-IR spectrum of carboxamide-*f*-GO, the C=O stretching frequencies of the amide bond formed by carboxamide functionalization appeared around 1720 cm^{-1} which indicate the attachment of carboxamide scaffolds on the surface of the GO (Fig. 1a). Also, the absorption of the N-H stretching of the amide is observed around 3200-3580 cm^{-1}. Furthermore, the bands at 2923 and 2854 cm^{-1} can be assigned to the asymmetric and symmetric methylene vibrations of cyclohexyl moiety. Finally, the peaks at 1041 cm^{-1} were attributed to the in-plane bending of C–H in benzene ring [49, 50]. The FT-IR spectrum of Cu NP-carboxamide-*f*-GO@Fe_3O_4 exhibits a broad band at 570 cm^{-1} corresponds to the stretching vibration of the Fe–O bonds

which attributed to the spinel form of Fe_3O_4 [51]. Notably, C=O stretching bonds show a slight shift to 1612 and 1566 cm^{-1} that could be due to the chelation of Cu NPs on the surface of carboxamide-*f*-GO (Fig. 1b).

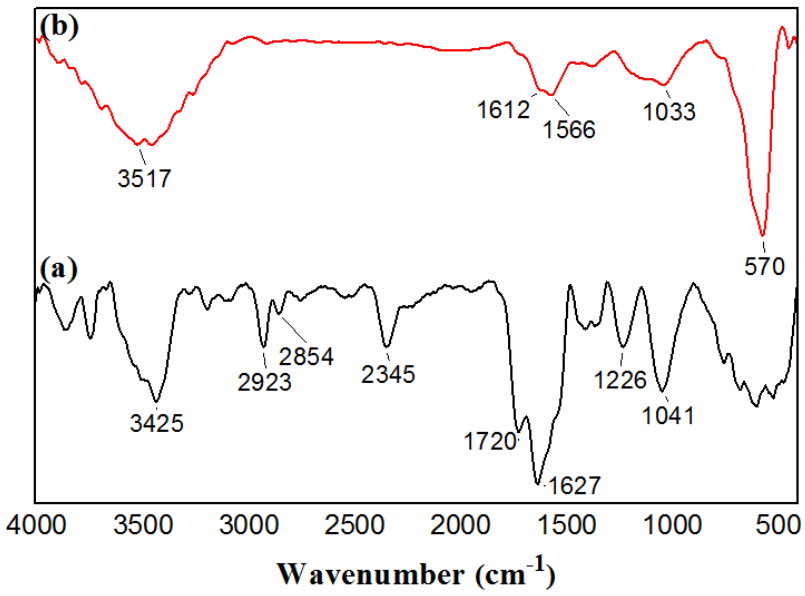

Figure 1 FT-IR spectra of carboxamide-*f*-GO (a) and Cu NP-carboxamide-*f*-GO@Fe_3O_4 (b)

One of the interesting features of this Ugi functionalization is the high dispersity and stability of the nanocomposite, more than one month, in water (Supporting Information, Fig. S2) and organic solvent. This stable dispersion in DMSO-d_6 caused to clear ^{1}H NMR spectrum. The nanocomposite spectrum shows a multiplet for the methylene protons of the cyclohexyl ring (δ = 1.16-1.71 ppm, 10H); a singlet for the methyl group of benzaldehyde (δ = 2.28 ppm, 3H), a multiplet for the NH−CH cyclohexyl (δ = 3.99-4.05 ppm, 1H); a singlet for methine proton of carboxamides (δ_H = 6.16 ppm, 1H), the aromatic protons gave rise to multiplets in the aromatic region of the spectrum (δ_H = 6.71−7.36 ppm, 5H) and a singlet for NH of amide group (δ_H = 7.83 ppm, 1H). The indication of protons of sp^3 carbons of cyclohexyl isocyanide along with methine proton of carboxamide scaffold obviously demonstrated the formation of Ugi-ligand on the surface of the graphene sheets (Fig. 2).

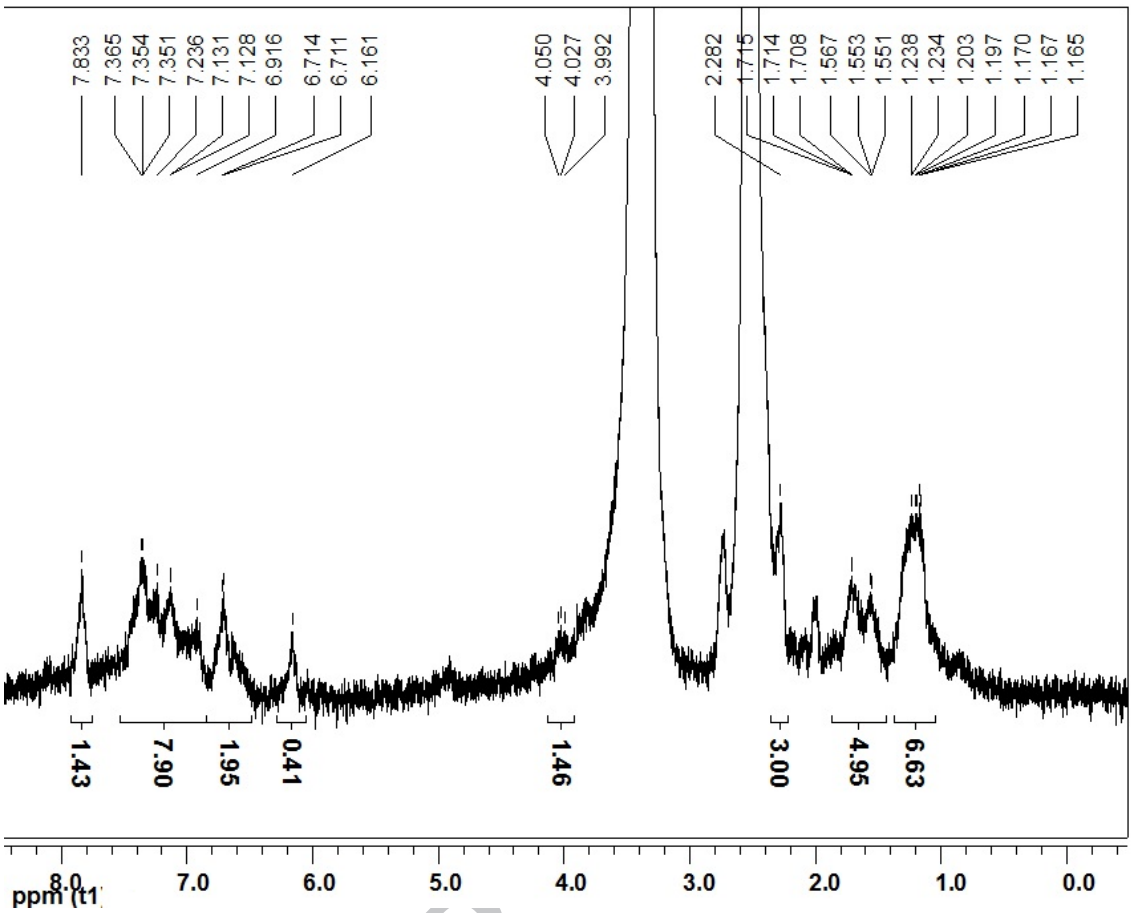

Figure 2 Representative ^{1}H NMR (DMSO-d_6) spectrum of carboxamide-*f*-GO

In a follow-up investigation for confirmation the ability of Ugi-4CR for the surface functionalization, the AFM images were obtained. AFM image of graphene (Fig. 3a) showed that the lateral width of the sheets was 300 ~ 600 nm and the thickness is about 2.5 nm. AFM image has revealed that the graphene is multilayered (2-4 layers), in comparison with reported AFM measurement which showed ~ 0.6-1 nm thickness for bare graphene [52, 53]. It can be seen from the AFM image of carboxamide-*f*-GO surface that graphene sheet fully covered with carboxamide functional groups leading to multi-layered functionalized graphene and increasing the thickness of sheets (Fig. 3b).

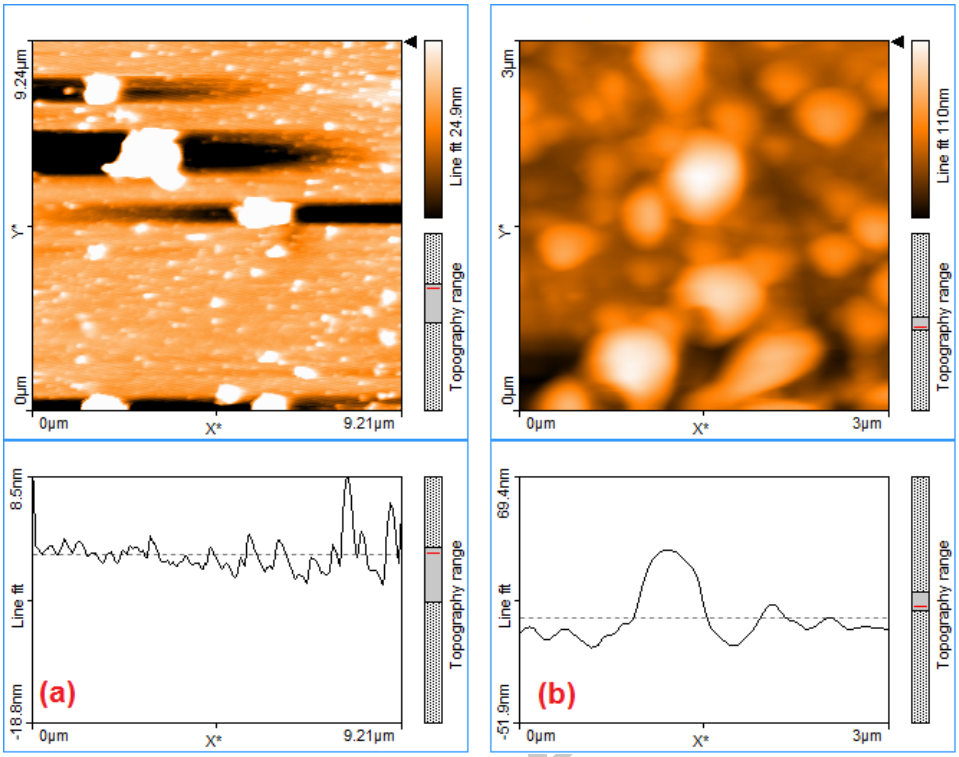

Figure 3. AFM images of graphene (a) and carboxamide-*f*-GO (b)

The XRD patterns of carboxamide-*f*-GO and Cu NP-carboxamide-*f*-GO@Fe_3O_4 are shown in Fig. 4. The pattern showed that the structure of the GO maintained uniformly through the Ugi reaction process because the diffraction peaks at 2θ =10.10 ° which were associated with the (001) interlayer spacing of 0.80 nm, were observed. Additionally, the peaks at 2θ= 44.14 ° and 64.42 ° correspond to stainless steel sample holder of powder diffractometer (Supporting Information, Fig. S3). In the XRD pattern of Cu NP-carboxamide-*f*-GO@Fe_3O_4, the peaks at 43.12°, 50.2° and 74.26° were assigned to the (111), (200) and (220) lattice planes of Cu NPs [54], and also the peaks at 30.04 ° , 35.44 °, 43.06 °, 53.62 °, 57.1°, and 62.62° corresponded to the (220), (311), (400), (422), (511), and (440) cubic spinel structure of the Fe_3O_4 NPs [55]. Cu NP-carboxamide-*f*-GO@Fe_3O_4 demonstrates broadened XRD traces, confirmed that it consists of nanocrystallites. Therefore, the average particle diameters were estimated using Scherrer's formula [55]. Calculation from full width at half maximum (FWHM) data using Scherrer's equation gave average crystallite size of 25.9 nm and 29.8 nm for Fe_3O_4 and Cu NPs, respectively.

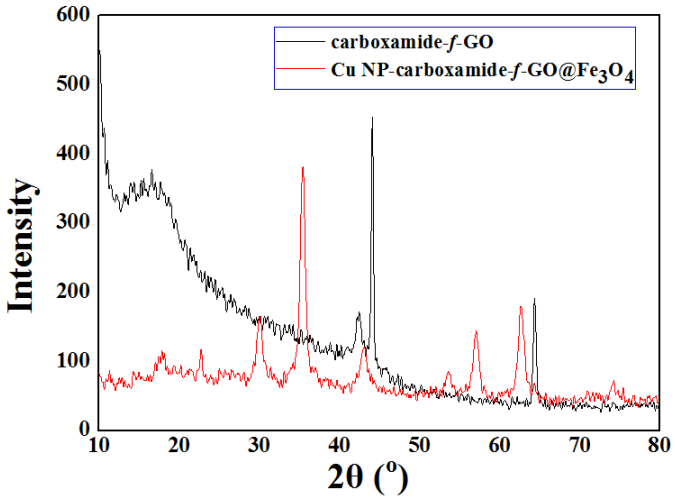

Figure 4 XRD patterns of carboxamide-*f*-GO and Cu NP-carboxamide-*f*-GO@Fe_3O_4

To gain insight into the structure and morphology of the nanocatalyst, the SEM images were obtained. The SEM image of GO shows the ultrathin homogeneous layered structure of the sheets (Fig. 5a). After functionalization *via* Ugi reaction and corporation of carboxamide scaffolds on the surface of the GO, SEM image confirms that the structure of GO was constantly remained. The mentioned result indicated that Ugi multicomponent reaction has a great potential for generating valuable functionalization on the surface of GO without any obvious changes in the structure and morphology during a facile one-pot procedure (Fig. 5b). In the case of Cu NP-carboxamide-*f*-GO@Fe_3O_4, the incorporation of Cu and Fe_3O_4 NPs with semispherical morphology was noticed (Fig. 5c). The components of carboxamide-*f*-GO and Cu NP-carboxamide-*f*-GO@Fe_3O_4 were determined by using energy dispersive (EDX) spectrometry. The EDX spectrum shows the elemental composition of (C, N and O) of carboxamide-*f*-GO and (O, Fe and Cu) of Cu NP-carboxamide-*f*-GO@Fe_3O_4 (Fig. 5d, e).

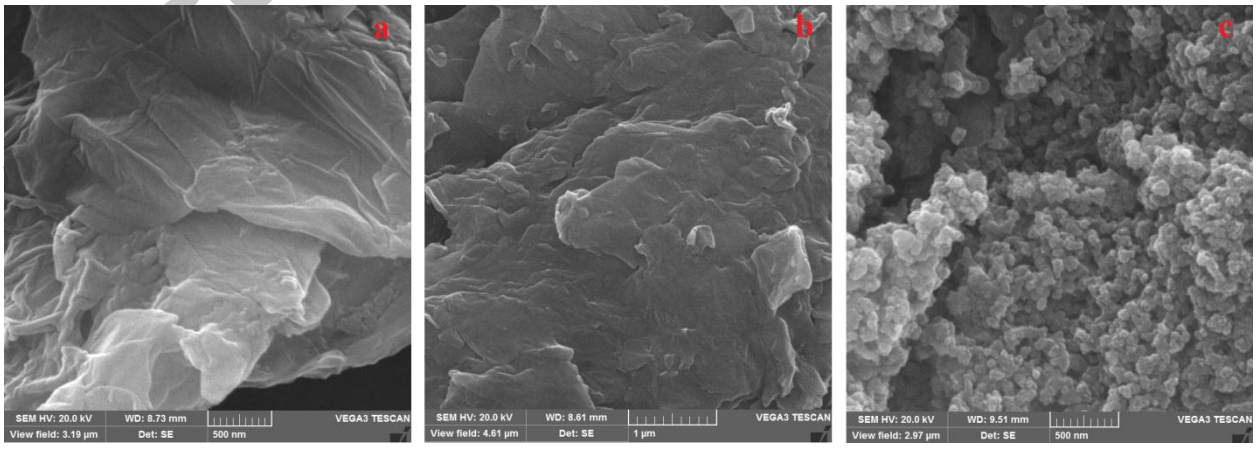

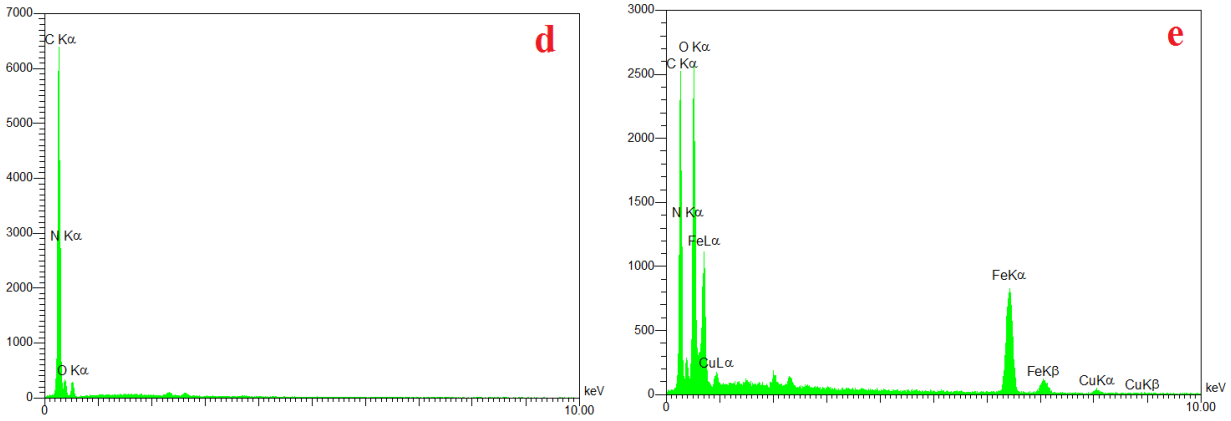

Figure 5 SEM images of: (a) GO, (b) carboxamide-*f*-GO, (c) Cu NP-carboxamide-*f*-GO@Fe_3O_4. EDX spectra of: (d) carboxamide-*f*-GO, (e) Cu NP-carboxamide-*f*-GO@Fe_3O_4

In this sense, an apparent hydrodynamic diameter of the nanocatalyst was measured with DLS analysis (Fig. 6). The DLS size measurement showed that the synthesized nanocatalyst had an average particle size range and polydispersity index (PdI) of 349 ±80 nm and 0.8±0.02, respectively. The nanocatalyst showed high polydispersity index which may due to the aggregation of graphene sheets and Fe_3O_4 NPs after functionalization [56]. On the basis of our literature survey, there is some report available on the covalent functionalization of graphene which showed similar high polydispersity index [57] and since the Cu NP-carboxamide-*f*-GO@Fe_3O_4 nanocomposites consist of different nanoparticles, the existence of distributions with differences in width is rational.

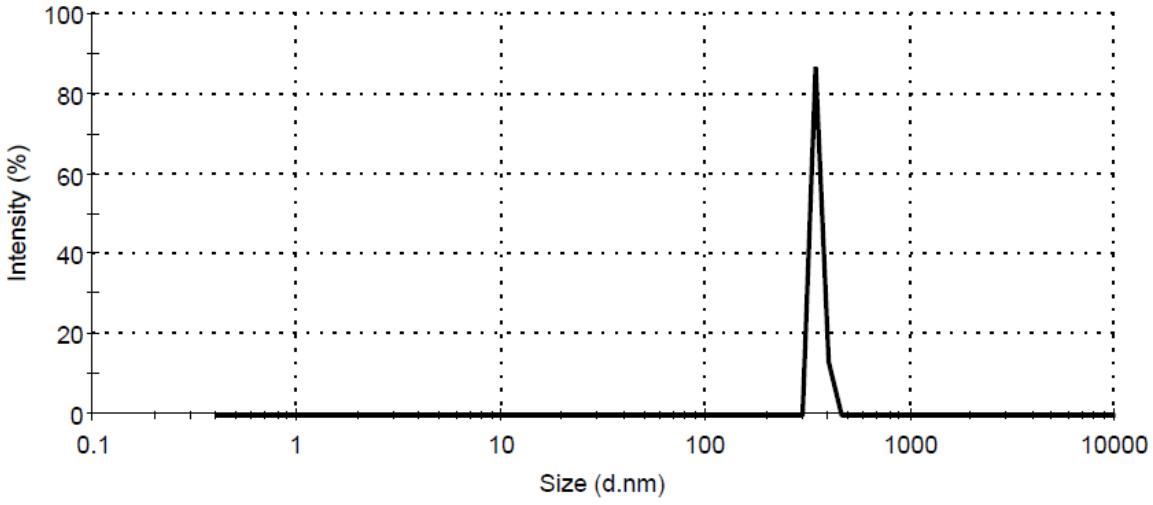

Figure 6. Particle size distribution of Cu NP-carboxamide-*f*-GO@Fe_3O_4 nanocatalyst

Thermal stability is one of the important factors for selecting an appropriate catalyst for the reaction, especially in the coupling reactions that need heating. Therefore, the thermal behavior of Cu NP-carboxamide-*f*-GO@Fe_3O_4 was characterized by thermogravimetric analysis and the TGA result is presented in Fig. 7. The weight loss from 120 °C to 220 °C is attributed to the decomposition of labile oxygen-containing functional groups which anchored to the surface of the graphene [58]. The weight loss from above 450 °C may ascribe to the pyrolysis and destruction of the graphite network [2]. The residual weight of ~ 17% presented the weight percentage of Cu and Fe_3O_4 NPs on the surface of functionalized GO.

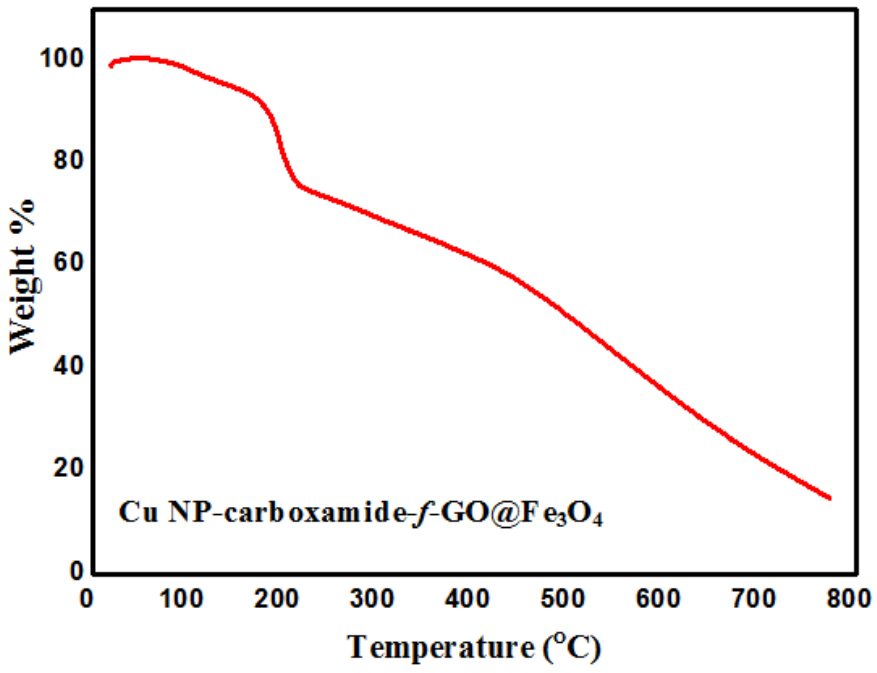

Figure 7. TGA curve of Cu NP-carboxamide-*f*-GO@Fe_3O_4 recorded at a heating rate of 10 °C min^{-1}

To demonstrate the catalytic activity of the synthesized Cu NP-carboxamide-*f*-GO@Fe_3O_4 nanocomposite, Ullmann C-N coupling of the *N*-heterocycles and primary amines with aryl halides have been investigated. For this purpose, the model reaction of 1-iodo-4-methoxybenzene **1b** and piperidine **2a** catalyzed by Cu NP-carboxamide-*f*-GO@Fe_3O_4 has performed for the synthesis of 1-(4-methoxyphenyl)piperidine (**3b)**. Likewise, the effects of engineering aspects, such as the temperature, solvent and bases on kinetics were investigated in detail. The initial experiments were carried out by running the model reaction in the presence of Cs_2CO_3 and K_2CO_3 as a base and 0.05 mol% of catalyst in different solvents. From Table 1, it is apparent that the solvent plays a significant role in the cross-coupling reaction. The reaction with K_2CO_3 as the base instead of Cs_2CO_3 in the DMF, DMSO and H_2O

caused to lower yield of **3b** (Table 1, Entries 1, 3 and 5). In continuation, due to the many advantages of deep eutectic solvent as a green medium in organic transformations and based on our interest in this medium [59-61], we used DES as a solvent in C-N cross-coupling Ullmann reaction. Subsequently, in the choline chloride-glycerol based DES no obvious difference in yields were observed when using Cs_2CO_3, and K_2CO_3 and since the K_2CO_3 is more available and cheaper than Cs_2CO_3, therefore K_2CO_3 in choline chloride-glycerol based DES was chosen under optimal conditions (Table 1, Entry 14). Even the yields in urea based DESs in the presence of the K_2CO_3 and NaOH are lower than glycerol-based DES (Table 1, Entries 8 and 9). The other acidic DESs showed very low yields for the Ullmann coupling reactions even after 3 hours (Table 1, Entries 10-12). In addition, several experiments were performed for the temperature optimization at 80 °C, 110 °C and 120 °C in the presence of K_2CO_3 in choline chloride-glycerol based DES utilizing 0.05 mol% Cu NP-carboxamide-*f*-GO@Fe_3O_4 (Table 1, Entries 14-16). As can be seen, the optimal reaction temperature is 110 ^oC (Entry 14 versus Entries 16 and 17). In the case of 80 °C, the yield of the coupling product was lower than the one at 110 °C. However, when the temperature increased to 120 °C, the yield of the coupling product did not increase significantly. It should be noted here that, in the absence of catalyst in optimum condition no coupling product could be detected (Table 1, Entry 17). The effect of catalyst loading was investigated using different quantities of the catalyst from 0.025 mol% to 0.1 mol% (Table 1, Entries 17, 19 and 20). At last but not least, Cu NP-carboxamide-*f*-GO@Fe_3O_4 (0.05 g) provided the best results at 110 °C in choline chloride-glycerol medium after 30 minutes.

Table 1. Optimization of the reaction conditions[a]

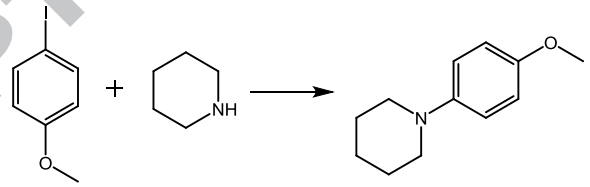

1b **2a** **3b**

Entry	Solvent	Base	Temp (^oC)	Time (h)	Yield (%)[b]
1	DMF	K_2CO_3	110	12	45
2	DMF	Cs_2CO_3	110	10	47
3	DMSO	K_2CO_3	110	5	70
4	DMSO	Cs_2CO_3	110	5	78
5	H_2O	K_2CO_3	Reflux	5	Trace
6	H_2O	Cs_2CO_3	Reflux	5	15

7	EtOH	K_2CO_3	Reflux	10	45
8	Choline chloride: urea (1:2)	NaOH	110	3	73
9	Choline chloride: urea (1:2)	K_2CO_3	110	3	68
10	Choline chloride: malonic acid (1:1)	K_2CO_3	110	3	Trace
11	Choline chloride: ethylene glycol (1:2)	K_2CO_3	110	3	20
12	Choline chloride: $FeCl_3$(1:3)	K_2CO_3	110	3	43
13	Choline chloride: citric acid (1:2)	NH_4Cl	110	3	72
14	Choline chloride: glycerol (1:2)	K_2CO_3	110	0.5	97
15	Choline chloride: glycerol (1:2)	Cs_2CO_3	110	0.5	98
16	Choline chloride: glycerol (1:2)	K_2CO_3	80	3	85
17	Choline chloride: glycerol (1:2)	K_2CO_3	120	3	97
18[c]	Choline chloride: glycerol (1:2)	K_2CO_3	110	3	No product
19[d]	Choline chloride: glycerol (1:2)	K_2CO_3	110	3	90
20[e]	Choline chloride: glycerol (1:2)	K_2CO_3	110	3	97

[a] Reaction conditions: 1-iodo-4-methoxybenzene (**1b**, 1 mmol, 0.23 g), piperidine (**2a**, 1 mmol, 0.08 g) and inorganic base (2 mmol) and catalyst (0.05 mol%);
[b] Isolated yield;
[c] In the absence of catalyst;
[d] Catalyst (0.025 mol%);
[e] Catalyst (0.1 mol%)

As is well known, reactions which possess the entropy-decreasing transformation are expedited by pressure. On the other hand, one of the most notable properties of DESs is their high viscosity which caused to creation of high-pressure cavities. This cavities formation may due to the many factors including the presence of an extensive hydrogen-bonding network, relatively large ion sizes, and electrostatic forces within the liquid [62]. Moreover, based on the hole theory, the viscosity of DESs corresponds to the holes available in the fluid which allows appropriate ionic motions [63]. On the basis of this theory, the volumetric factors are more effective than interactions between a salt and a hydrogen-bonding donor [64]. The presence of these high pressure cavities which undergoes the reactions that associated with decreasing of the entropy and high thermal stability [65] have set DES as an appropriate medium for organic reactions under high pressure and temperature besides being environmentally benign media. Since, C-N coupling reactions associated with negative activation volumes and entropy decreasing owing to the conversion of two substrates to one molecule of compound, therefore the choice of deep eutectic solvent for coupling reactions is very rational. Our results in Table 1 unveil a clear correlation between the high pressure choline chloride-glycerol based DES and C-N cross-coupling reaction for providing the coupling product with high yield in the low reaction time, suggesting that extensive hydrogen-bonding network of choline chloride-glycerol based DES creating strain inside its cavity and so

promote the coupling reaction efficiency. In addition, it can be concluded that the presence of the synthesized nanocatalyst along with DES caused the synergistic effects to promote the Ullman C-N cross-coupling significantly. Since glycerol is readily available and has low toxicity, it could be a great candidate for combining with choline chloride to produce an ideal eco-friendly medium for the syntheses that need high pressure [48].

After optimizing the reaction conditions, to study generality of the Cu NP-carboxamide-*f*-GO@Fe_3O_4 nanocomposite in the C-N Ullmann coupling reaction, the reaction was extended to *N*-heterocycles and diverse anilines with various types of aryl halides in obtained optimized conditions. Aryl halides containing electron-deficient and electron-rich groups were found to react efficiently with good to excellent yields. Also, various secondary cyclic amines such as morpholine, 1,2,3,4-tetrahydroisoquinoline and piperidine and heterocyclic nitrogen compounds for examples, imidazole and benzimidazole along with different anilines have been applied to obtain the desired products with good yields (Table 2).

Table 2. *N*-arylation of amines catalyzed *via* Cu NP-carboxamide-*f*-GO@Fe_3O_4 nanocomposite in DES

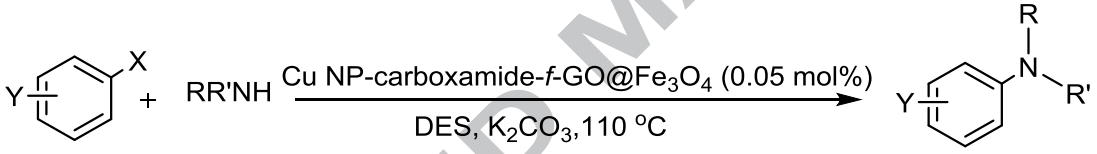

Entry	Aryl Halide	Amine	Product	Yield (%)[a]
1	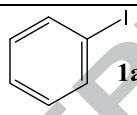 **1a**	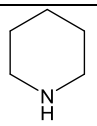 **2a**	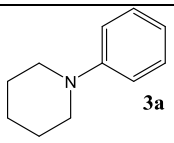 **3a**	90
2	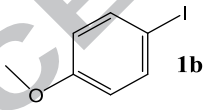 **1b**	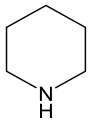 **2a**	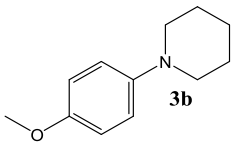 **3b**	97
3	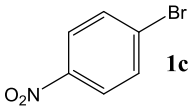 **1c**	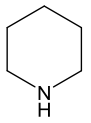 **2a**	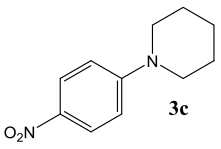 **3c**	95
4	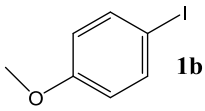 **1b**	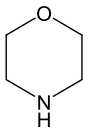 **2b**	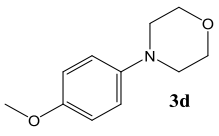 **3d**	97

5	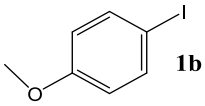	**1b**	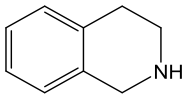	**2c**	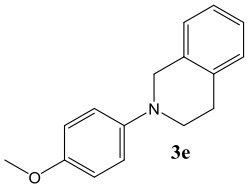 **3e**	75
6	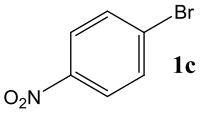	**1c**	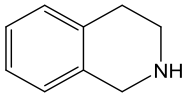	**2c**	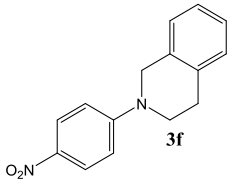 **3f**	80
7	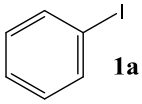	**1a**	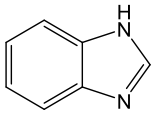	**2d**	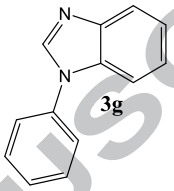 **3g**	99
8	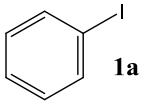	**1a**	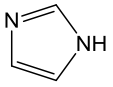	**2e**	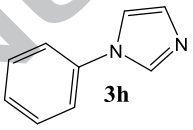 **3h**	91
9	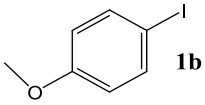	**1b**	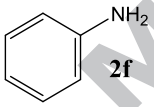	**2f**	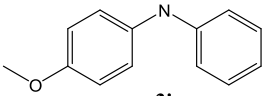 **3i**	78
10	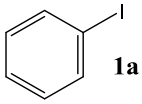	**1a**	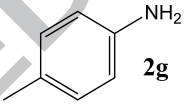	**2g**	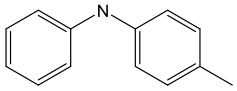 **3j**	83
11	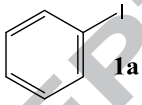	**1a**	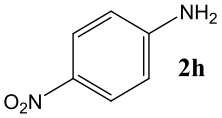	**2h**	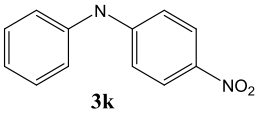 **3k**	76
12	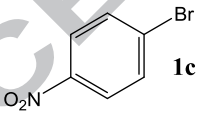	**1c**	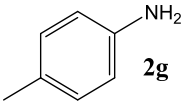	**2g**	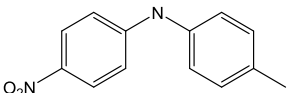 **3l**	93

[a] Isolated yield

The efficiency of the synthesized nanocatalyst in comparison with the other reported catalysts is given in Table 3. The results indicated that in the case of Cu NP-carboxamide-*f*-GO@Fe_3O_4, the reaction yield is rather increased at the relatively shorter reaction times. In addition, the Cu percent is much lower than the other nanocatalysts. By contrast, DES medium shows a great efficiency as a green solvent toward this synthesis while having an outstanding advantage of eco-compatibility.

Table 3. Comparing the catalytic efficiency of various copper catalysts in *N*-arylation of amines

Entry	Catalyst	Reaction conditions	Time (h)	Yield (%)	Ref.
1	CuBr/DPPhen (5 mol%)	H_2O, PEG-400 (20 mol%), KOH, 100 ^oC	21-48	74-97	[66]
2	CuI (10 mol%)	DMSO, CsF (2 equiv.), 130 ^oC, N_2	24	37-94	[67]
3	CuO NPs (5 mol%)	DMSO/*t*-BuOH, KOH, 110 ^oC	-	10-89	[68]
4	MOF-199	DMSO, NaOH, 120 ^oC	12	50-97	[69]
5	Activated-Cu (10 mol%)	H_2O, LiOH, TBAB, 120 ^oC	24	35-81	[70]
6	CuO/MWCNT (0.98 mol%)	DMAc, K_2CO_3,120 ^oC	24	47-96	[71]
7	Cu NP-carboxamide-*f*-GO@Fe_3O_4 (0.05 mol%)	DES, K_2CO_3 ,110 ^oC	0.5-3	75-99	**This work**

The possibility of recycling is one of the advantages of heterogeneous catalyst systems from the green chemistry point of view. Additionally, it should be noted here that one of the distinct advantages of DES medium is its ability to perform as a recyclable reaction media. Therefore, in the present designed strategy, not only the catalyst can be recycled with the external magnet, but also the DES medium can be recovered even for five consecutive runs with no considerable loss of catalytic activity. In order to establish the reusability of the nanocatalyst and DES, the reaction of 1-iodo-4-methoxybenzene **1b** and piperidine **2a** as a model reaction was repeated under optimal conditions (Table 2, Entry 2). When the reaction was completed, DES was dissolved in water, the Cu NP-carboxamide-*f*-GO@Fe_3O_4 nanocatalyst was readily separated by an external magnet and the crude product was filtered. Then the DES was recovered by evaporating water at 80 °C under vacuum and recycled with nanocatalyst for the next experiment. For each run, three independent experiments were performed. The data points in Fig. 8 are the average of three independent experiments. Error bars represent the range over which the values were observed. The results reveal that only minor decreases in the reaction yields are observed and the recovered catalyst and medium retained a significant fraction of the original activity.

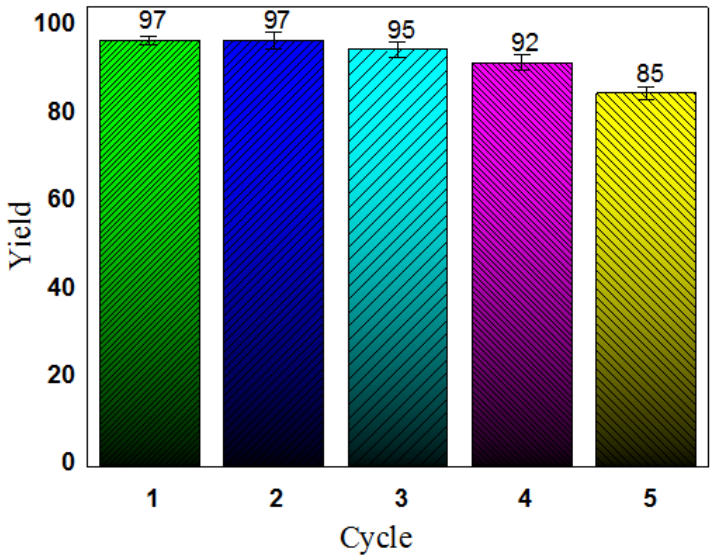

Figure 8. Reusability of the nanocatalyst and DES for Ullman C-N coupling reaction

Conclusion

In conclusion, we present a "new" horizon of the "old" Ugi reaction in material science for the synthesis of affinity ligands on the surface of graphene oxide sheets. This work provides new prospects not only in the functionalization of carbonaceous materials with multicomponent reactions (MCRs), but also in the application of the as-prepared nanocomposite for high yield C-N Ullmann coupling reactions in a DES as a green medium and alternative choice for toxic organic solvents. In this context, a copper nanoparticle modified carboxamide-functionalized magnetic graphene oxide nanocatalyst has been synthesized *via* a one-pot four component Ugi reaction. The Ugi-ligand with carboxamide motifs can act as an efficient ligand with high affinity toward copper nanoparticles. It is worth noting that the utilization of DES instead of the conventional toxic solvents such as toluene, DMF and DMSO in coupling reactions is in resonance with the state of the art. The advantages of using this environmentally benign and facile catalytic route are easy workup, high yield, being eco-friendly and moreover, shortened reaction times as the greatest exclusivity of this system. In addition, complexation of the Ugi-ligand to the copper prevents leaching and agglomeration of nanoparticles and improves reusability of the heterogeneous catalyst. The Cu NP-carboxamide-*f*-GO@Fe_3O_4 nanocomposite and DES were easily recovered and reused for five consecutive runs. Consequently, these results broaden the scope of using this catalyst as an adequate platform in the other heterogeneous catalytic transformations. In addition, along with a growing demand on the utilization of functional materials in a wide spectrum of interdisciplinary applications, it seems that different MCRs can be great candidates for material functionalization. Since, time-consuming, different

purification steps and exhausting chemical transformations are not necessary and even non-experts can synthesize functionalized materials, therefore these functionalization systems can shift from laboratory to industry. Efforts are underway to functionalization of carbonaceous materials with the other important MCRs for drug delivery applications and catalytic routes.

Acknowledgments

We gratefully acknowledge financial support from the Iran National Science Foundation (INSF) and the Research Council of Shahid Beheshti University.

References

[1] A.K. Geim, K.S. Novoselov, The rise of graphene, Nat. Mater., 6 (2007) 183-191.
[2] K.S. Novoselov, A.K. Geim, S.V. Morozov, D. Jiang, Y. Zhang, S.V. Dubonos, I.V. Grigorieva, A.A. Firsov, Electric field effect in atomically thin carbon films, Science, 306 (2004) 666-669.
[3] A.C. Neto, F. Guinea, N.M. Peres, K.S. Novoselov, A.K. Geim, The electronic properties of graphene, Rev. Mod. Phys., 81 (2009) 109.
[4] C. Lee, X. Wei, J.W. Kysar, J. Hone, Measurement of the elastic properties and intrinsic strength of monolayer graphene, Science, 321 (2008) 385-388.
[5] R.R. Salunkhe, Y.H. Lee, K.H. Chang, J.M. Li, P. Simon, J. Tang, N.L. Torad, C.C. Hu, Y. Yamauchi, Nanoarchitectured graphene-based supercapacitors for next-generation energy-storage applications, Chem. Eur. J. 20 (2014) 13838-13852.
[6] J. Tang, Y. Yamauchi, Carbon materials: MOF morphologies in control, Nat. Chem., 8 (2016) 638-639.
[7] R.R. Salunkhe, S.H. Hsu, K.C. Wu, Y. Yamauchi, Large-Scale Synthesis of Reduced Graphene Oxides with Uniformly Coated Polyaniline for Supercapacitor Applications, ChemSusChem, 7 (2014) 1551-1556.
[8] S. Stankovich, D.A. Dikin, G.H. Dommett, K.M. Kohlhaas, E.J. Zimney, E.A. Stach, R.D. Piner, S.T. Nguyen, R.S. Ruoff, Graphene-based composite materials, Nature, 442 (2006) 282-286.
[9] A.A. Balandin, Thermal properties of graphene and nanostructured carbon materials, Nat. Mater., 10 (2011) 569-581.
[10] Y. Zhu, S. Murali, W. Cai, X. Li, J.W. Suk, J.R. Potts, R.S. Ruoff, Graphene and graphene oxide: synthesis, properties, and applications, Adv. Mater., 22 (2010) 3906-3924.
[11] J. Pyun, Graphene oxide as catalyst: application of carbon materials beyond nanotechnology, Angew. Chem. Int. Ed., 50 (2011) 46-48.
[12] J. Liu, L. Cui, D. Losic, Graphene and graphene oxide as new nanocarriers for drug delivery applications, Acta Biomater., 9 (2013) 9243-9257.
[13] Y. Shao, J. Wang, H. Wu, J. Liu, I.A. Aksay, Y. Lin, Graphene based electrochemical sensors and biosensors: a review, Electroanalysis, 22 (2010) 1027-1036.
[14] Z. Hu, Y. Zhao, J. Liu, J. Wang, B. Zhang, X. Xiang, Ultrafine MnO 2 nanoparticles decorated on graphene oxide as a highly efficient and recyclable catalyst for aerobic oxidation of benzyl alcohol, J. Colloid Interface Sci., 483 (2016) 26-33.
[15] S.K. Singh, M.K. Singh, P.P. Kulkarni, V.K. Sonkar, J.J. Grácio, D. Dash, Amine-modified graphene: thrombo-protective safer alternative to graphene oxide for biomedical applications, ACS Nano, 6 (2012) 2731-2740.
[16] D.R. Dreyer, S. Park, C.W. Bielawski, R.S. Ruoff, The chemistry of graphene oxide, Chem. Soc. Rev., 39 (2010) 228-240.

[17] T. Ramanathan, A. Abdala, S. Stankovich, D. Dikin, M. Herrera-Alonso, R. Piner, D. Adamson, H. Schniepp, X. Chen, R. Ruoff, Functionalized graphene sheets for polymer nanocomposites, Nat. Nanotechnol., 3 (2008) 327-331.
[18] V. Georgakilas, J.N. Tiwari, K.C. Kemp, J.A. Perrnan, A.B. Bourlinos, K.S. Kim, R. Zboril, Noncovalent functionalization of graphene and graphene oxide for energy materials, biosensing, catalytic, and biomedical applications, Chem. Rev., 9 (2016) 5464–5519.
[19] C. Zhang, R. Hao, H. Liao, Y. Hou, Synthesis of amino-functionalized graphene as metal-free catalyst and exploration of the roles of various nitrogen states in oxygen reduction reaction, Nano Energy, 2 (2013) 88-97.
[20] Q. Yang, X. Pan, K. Clarke, K. Li, Covalent functionalization of graphene with polysaccharides, Ind. Eng. Chem. Res., 51 (2011) 310-317.
[21] T. Kuila, S. Bose, A.K. Mishra, P. Khanra, N.H. Kim, J.H. Lee, Chemical functionalization of graphene and its applications, Prog. Mater Sci., 57 (2012) 1061-1105.
[22] V. Georgakilas, M. Otyepka, A.B. Bourlinos, V. Chandra, N. Kim, K.C. Kemp, P. Hobza, R. Zboril, K.S. Kim, Functionalization of graphene: covalent and non-covalent approaches, derivatives and applications, Chem. Rev., 112 (2012) 6156-6214.
[23] Í.L. Batalha, A.C. Roque, Petasis-Ugi ligands: New affinity tools for the enrichment of phosphorylated peptides, J. Chromatogr. B, 1031 (2016) 86-93.
[24] S.L. Jain, P. Bhattacharyya, H.L. Milton, A.M. Slawin, J.A. Crayston, J.D. Woollins, New pyridine carboxamide ligands and their complexation to copper (II). X-Ray crystal structures of mono-, di, tri-and tetranuclear copper complexes, Dalton Trans., 0 (2004) 862-871.
[25] C.A. Lesburg, C.-c. Huang, D.W. Christianson, C.A. Fierke, Histidine→ carboxamide ligand substitutions in the zinc binding site of carbonic anhydrase II alter metal coordination geometry but retain catalytic activity, Biochemistry, 36 (1997) 15780-15791.
[26] S. Mallakpour, A. Abdolmaleki, A. Karshenas, Graphene oxide supported copper coordinated amino acids as novel heterogeneous catalysts for epoxidation of norbornene, Catal. Commun., 92 (2017) 109-113.
[27] A. Domling, The Discovery of New Isocyanide-Based Multicomponent Reactions, ChemInform, 31 (2000).
[28] A. Shaabani, S.E. Hooshmand, Isocyanide and Meldrum's acid-based multicomponent reactions in diversity-oriented synthesis: from a serendipitous discovery towards valuable synthetic approaches, RSC Adv., 6 (2016) 58142-58159.
[29] J. Alemán, S. Cabrera, C. Alvarado, Recent Advances in the Ugi Multicomponent Reactions, Multicomponent Reactions, John Wiley & Sons, Inc2015, pp. 247-282.
[30] C. Hebach, U. Kazmaier, Via Ugi reactions to conformationally fixed cyclic peptides, Chem. Commun., 0 (2003) 596-597.
[31] G. Koopmanschap, E. Ruijter, R.V. Orru, Isocyanide-based multicomponent reactions towards cyclic constrained peptidomimetics, Beilstein J. Org. Chem., 10 (2014) 544-598.
[32] A. Rezaei, O. Akhavan, E. Hashemi, M. Shamsara, Toward Chemical Perfection of Graphene-Based Gene Carrier via Ugi Multicomponent Assembly Process, Biomacromolecules, 17 (2016) 2963-2971.
[33] A. Rezaei, O. Akhavan, E. Hashemi, M. Shamsara, Ugi Four Component Assembly Process: An Efficient Approach for One-pot Multi-functionalization of Nano Graphene Oxide in Water and Their Application in Lipase Immobilization, Chem. Mater., 9 (2016) 3004–3016.
[34] A. Shaabani, R. Afshari, Synthesis of Carboxamide-Functionalized Multiwall Carbon Nanotubes via Ugi Multicomponent Reaction: Water-Dispersible Peptidomimetic Nanohybrid as Controlled Drug Delivery Vehicle, ChemistrySelect, 2 (2017) 5218-5225.
[35] H. Li, C. Li, J. Bai, C. Zhang, W. Sun, Carbon nanofiber supported copper nanoparticles catalyzed Ullmann-type coupling reactions under ligand-free conditions, RSC Adv., 4 (2014) 48362-48367.

[36] L. Rout, S. Jammi, T. Punniyamurthy, Novel CuO nanoparticle catalyzed C− N cross coupling of amines with iodobenzene, Org. Lett., 9 (2007) 3397-3399.
[37] M. Nasrollahzadeh, S.M. Sajadi, A. Rostami-Vartooni, S.M. Hussin, Green synthesis of CuO nanoparticles using aqueous extract of Thymus vulgaris L. leaves and their catalytic performance for N-arylation of indoles and amines, J. Colloid Interface Sci., 466 (2016) 113-119.
[38] A.P. Abbott, G. Capper, D.L. Davies, R.K. Rasheed, V. Tambyrajah, Novel solvent properties of choline chloride/urea mixtures, Chem. Commun., DOI (2003) 70-71.
[39] Q. Zhang, K.D.O. Vigier, S. Royer, F. Jérôme, Deep eutectic solvents: syntheses, properties and applications, Chem. Soc. Rev., 41 (2012) 7108-7146.
[40] E.L. Smith, A.P. Abbott, K.S. Ryder, Deep eutectic solvents (DESs) and their applications, Chem. Rev., 114 (2014) 11060-11082.
[41] M.K. AlOmar, M.A. Alsaadi, T.M. Jassam, S. Akib, M.A. Hashim, Novel deep eutectic solvent-functionalized carbon nanotubes adsorbent for mercury removal from water, J. Colloid Interface Sci., 497 (2017) 413-421.
[42] A. Shaabani, R. Afshari, S.E. Hooshmand, A.T. Tabatabaei, F. Hajishaabanha, Copper supported on MWCNT-guanidine acetic acid@ Fe 3 O 4: synthesis, characterization and application as a novel multi-task nanocatalyst for preparation of triazoles and bis (indolyl) methanes in water, RSC Adv., 6 (2016) 18113-18125.
[43] M. Mahyari, M.S. Laeini, A. Shaabani, Aqueous aerobic oxidation of alkyl arenes and alcohols catalyzed by copper (II) phthalocyanine supported on three-dimensional nitrogen-doped graphene at room temperature, Chem. Commun., 50 (2014) 7855-7857.
[44] A. Shaabani, R. Afshari, S.E. Hooshmand, The crosslinked chitosan nanoparticles-anchored magnetic multi-wall carbon nanotubes: A bio-nanoreactor with extremely high activity toward click-multi-component reactions, New J. Chem., 41 (2017) 8469-8481.
[45] S. Shaabani, A. Shaabani, S.W. Ng, One-pot synthesis of coumarin-3-carboxamides containing a triazole ring via an isocyanide-based six-component reaction, ACS. Comb. Sci., 16 (2014) 176-183.
[46] A. Shaabani, S.E. Hooshmand, Diversity-oriented catalyst-free synthesis of pseudopeptides containing rhodanine scaffolds via a one-pot sequential isocyanide-based six-component reactions in water using ultrasound irradiation, Ultrason. Sonochem., 40 (2017) 84-90.
[47] Y. Liu, P. Liu, Z. Su, F. Li, F. Wen, Attapulgite–Fe 3 O 4 magnetic nanoparticles via co-precipitation technique, Appl. Surf. Sci., 255 (2008) 2020-2025.
[48] A.P. Abbott, R.C. Harris, K.S. Ryder, C. D'Agostino, L.F. Gladden, M.D. Mantle, Glycerol eutectics as sustainable solvent systems, Green Chem., 13 (2011) 82-90.
[49] H. Günzler, H.-U. Gremlich, IR spectroscopy. An introduction, Wiley-VSH; Inc, 2002, pp.223–227.
[50] A. Rezaei, O. Akhavan, E. Hashemi, M. Shamsara, Ugi four-component assembly process: An efficient approach for one-pot multifunctionalization of nanographene oxide in water and its application in lipase immobilization, Chem. Mater., 28 (2016) 3004-3016.
[51] R.N. Baig, R.S. Varma, Organic synthesis via magnetic attraction: benign and sustainable protocols using magnetic nanoferrites, Green Chem., 15 (2013) 398-417.
[52] D. Berman, A. Erdemir, A.V. Zinovev, A.V. Sumant, Nanoscale friction properties of graphene and graphene oxide, Diamond Relat. Mater., 54 (2015) 91-96.
[53] S.A. Han, K.H. Lee, T.-H. Kim, W. Seung, S.K. Lee, S. Choi, B. Kumar, R. Bhatia, H.-J. Shin, W.-J. Lee, Hexagonal boron nitride assisted growth of stoichiometric Al 2 O 3 dielectric on graphene for triboelectric nanogenerators, Nano Energy, 12 (2015) 556-566.
[54] N.A. Dhas, C.P. Raj, A. Gedanken, Synthesis, characterization, and properties of metallic copper nanoparticles, Chem. Mater., 10 (1998) 1446-1452.
[55] S. Sun, H. Zeng, Size-controlled synthesis of magnetite nanoparticles, J. Am. Chem. Soc., 124 (2002) 8204-8205.

[56] S.S. Rane, P. Choi, Polydispersity Index: How Accurately Does It Measure the Breadth of the Molecular Weight Distribution?, Chem. Mater., 17 (2005) 926-926.
[57] S. Stankovich, R.D. Piner, S.T. Nguyen, R.S. Ruoff, Synthesis and exfoliation of isocyanate-treated graphene oxide nanoplatelets, Carbon, 44 (2006) 3342-3347.
[58] S. Stankovich, D.A. Dikin, R.D. Piner, K.A. Kohlhaas, A. Kleinhammes, Y. Jia, Y. Wu, S.T. Nguyen, R.S. Ruoff, Synthesis of graphene-based nanosheets via chemical reduction of exfoliated graphite oxide, carbon, 45 (2007) 1558-1565.
[59] A. Shaabani, S.E. Hooshmand, M.T. Nazeri, R. Afshari, S. Ghasemi, Deep eutectic solvent as a highly efficient reaction media for the one-pot synthesis of benzo-fused seven-membered heterocycles, Tetrahedron Lett., 57 (2016) 3727-3730.
[60] A. Shaabani, S.E. Hooshmand, Choline chloride/urea as a deep eutectic solvent/organocatalyst promoted three-component synthesis of 3-aminoimidazo-fused heterocycles via Groebke–Blackburn–Bienayme process, Tetrahedron Lett., 57 (2016) 310-313.
[61] A. Shaabani, R. Afshari, S.E. Hooshmand, Passerini three-component cascade reactions in deep eutectic solvent: an environmentally benign and rapid system for the synthesis of α-acyloxyamides, Res. Chem. Intermed., 42 (2016) 5607-5616.
[62] T. Arnold, A.J. Jackson, A. Sanchez-Fernandez, D. Magnone, A.E. Terry, K.J. Edler, Surfactant Behavior of Sodium Dodecylsulfate in Deep Eutectic Solvent Choline Chloride/Urea, Langmuir, 31 (2015) 12894-12902.
[63] A.P. Abbott, G. Capper, S. Gray, Design of improved deep eutectic solvents using hole theory, ChemPhysChem, 7 (2006) 803-806.
[64] S. Sarmad, J.-P. Mikkola, X. Ji, Carbon Dioxide Capture with Ionic Liquids and Deep Eutectic Solvents: A New Generation of Sorbents, ChemSusChem, 10 (2017) 324-352.
[65] H.G. Morrison, C.C. Sun, S. Neervannan, Characterization of thermal behavior of deep eutectic solvents and their potential as drug solubilization vehicles, Int. J. Pharm., 378 (2009) 136-139.
[66] J. Engel-Andreasen, B. Shimpukade, T. Ulven, Selective copper catalysed aromatic N-arylation in water, Green Chem., 15 (2013) 336-340.
[67] I. Güell, X. Ribas, Ligand-Free Ullmann-Type C–Heteroatom Couplings Under Practical Conditions, Eur. J. Org. Chem., 2014 (2014) 3188-3195.
[68] S. Jammi, S. Sakthivel, L. Rout, T. Mukherjee, S. Mandal, R. Mitra, P. Saha, T. Punniyamurthy, CuO nanoparticles catalyzed C− N, C− O, and C− S cross-coupling reactions: Scope and mechanism, J. Org. Chem, 74 (2009) 1971-1976.
[69] Z. Li, F. Meng, J. Zhang, J. Xie, B. Dai, Efficient and recyclable copper-based MOF-catalyzed N-arylation of N-containing heterocycles with aryliodides, Org. Biomol. Chem., 14 (2016) 10861-10865.
[70] Q. Yang, Y. Wang, D. Lin, M. Zhang, N-arylation of heterocycles catalyzed by activated-copper in pure water, Tetrahedron Lett., 54 (2013) 1994-1997.
[71] M. Gopiraman, S.G. Babu, Z. Khatri, W. Kai, Y.A. Kim, M. Endo, R. Karvembu, I.S. Kim, An efficient, reusable copper-oxide/carbon-nanotube catalyst for N-arylation of imidazole, Carbon, 62 (2013) 135-148.

Graphical abstract